

# Advancing Residual Learning towards Powerful Deep Spiking Neural Networks

Yifan Hu , Yujie Wu , Lei Deng and Guoqi Li

Department of Precision Instrument, Tsinghua University

## Abstract

Despite the rapid progress of neuromorphic computing, inadequate capacity and insufficient representation power of spiking neural networks (SNNs) severely restrict their application scope in practice. Residual learning and shortcuts have been evidenced as an important approach for training deep neural networks, but rarely did previous work assess their applicability to the characteristics of spike-based communication and spatiotemporal dynamics. In this paper, we first identify that this negligence leads to impeded information flow and accompanying degradation problem in previous residual SNNs. Then we propose a novel SNN-oriented residual block, MS-ResNet, which is able to significantly extend the depth of directly trained SNNs, e.g. up to 482 layers on CIFAR-10 and 104 layers on ImageNet, without observing any slight degradation problem. We validate the effectiveness of MS-ResNet on both frame-based and neuromorphic datasets, and MS-ResNet104 achieves a superior result of 76.02% accuracy on ImageNet, the first time in the domain of directly trained SNNs. Great energy efficiency is also observed that on average only one spike per neuron is needed to classify an input sample. We believe our powerful and scalable models will provide a strong support for further exploration of SNNs.

## 1 Introduction

Spiking neural networks are a typical kind of brain-inspired models with their unique features of rich neuronal dynamics and diverse coding schemes. Different from traditional artificial neural networks (ANNs), SNNs are capable of encoding information in spatiotemporal dynamics and using asynchronous binary spiking activities for event-driven communication. Recent progress in neuromorphic computing has demonstrated their great energy efficiency [Pei *et al.*, 2019; Mayr *et al.*, 2019; Akopyan *et al.*, 2015; Davies *et al.*, 2018]. Theoretically, SNNs are at least as computationally powerful as ANNs and the universal approximation theorem also applies to SNNs [Maass, 1997], so it is not surprising that SNNs

have been reported in various domains, such as image classification [Wu *et al.*, 2019], object detection [Kim *et al.*, 2020] and tracking [Yang *et al.*, 2019], speech recognition [Wu *et al.*, 2020], light-flow estimation [Lee *et al.*, 2020], and so forth. However, the status quo of deficiency in powerful SNN models seriously limits their capabilities for complex tasks in practice.

Conversion from a pre-trained model and surrogate gradient-based direct training are two mainstream approaches for obtaining an high-accuracy SNN model. The conversion method is free of the dilemma caused by the non-differentiable spiking activation function and can implement the inference of deep SNNs with tens or even hundreds of layers depending on the pre-trained ANN models adopted [Sengupta *et al.*, 2019; Han *et al.*, 2020; Hu *et al.*, 2018; Stöckl and Maass, 2021]. Although comparable accuracy to the pre-trained models can be achieved, the method treats SNNs more as an alternative expression of ANNs, and hundreds of time steps are usually required to achieve a satisfying conversion loss. It thereby fails to achieve low-latency computation in practical applications. The latter method utilizes a surrogate gradient function to enable backpropagation (BP) through time in the direct training of SNNs. The networks learn to encode information effectively and consequently only need much fewer time steps than the conversion ones. In addition, they are inherently more suited for processing spatiotemporal data from the emerging AER-based (address-event-representation) sensors, where the pre-training of ANNs is usually not applicable.

Unfortunately, one prominent problem of the directly trained SNNs lies in the limited scale of models. Earlier works mainly focus on shallow structures and simple tasks, such as MNIST [Deng, 2012]. Inspired from the representation power of deep ANNs, recent works have gradually evolved from fully-connected networks to convolutional networks to more advanced ResNet, for example Zheng *et al.* report the successful training of spiking ResNet-34 on ImageNet. However, the plain transplantation of the canonical ResNet, a way almost all previous works have adopted, does not work appropriately for the training of SNNs and the symptom will manifest itself in our depth-analysis experiments as an accuracy drop on both the training and test sets as the network deepens, which is named the degradation problem. As a result, building a deeper SNN still appears to be

arduous and fruitless. To this end, a specific residual block design is highly desirable for applying deep residual learning to SNNs.

We summarize our major contributions in this work as follows:

- We report the degradation problem when applying the vanilla ResNet in deep SNN training, and reveal the implicit unavailing residual representation and unstable gradient norm in the structure.
- We design a novel alternative residual block, MS-ResNet, which enables us to significantly extend the depth of directly trained SNNs, e.g., up to 482 layers on CIFAR-10 and 104 layers on ImageNet, without slight degradation problem.
- We evaluate the effectiveness of our methods on various datasets and obtain accuracy results which are, to the best of our knowledge, much better than previous work in directly trained SNNs and competitive to the conversion methods via extremely fewer time steps. Along with the binary and sparse spiking activities, great energy efficiency is also validated in an operation-based estimation.

## 2 Related Works

### 2.1 SNN Training Algorithms

There are two main routines to training an high-accuracy SNN model. The first is the conversion method. Its basic idea is that the continuous activation values in an ANN using ReLU can be approximated by the average firing rate of an SNN under the rate coding scheme. After training an ANN with certain structure restrictions and the BP algorithm, it is feasible to convert the pre-trained ANN into its spiking counterpart. Conversion-based SNNs maintain the smallest gap with ANNs in terms of accuracy and can be generalized to large-scale structures, such as VGG and ResNet [Rueckauer *et al.*, 2017; Hu *et al.*, 2018; Stöckl and Maass, 2021]. However, the conversion method also has its inherent defects. An accuracy gap will be caused by the constraints on ANN models and a long simulation duration with hundreds or thousands of time steps is required to complete an inference, which leads to extra delay and energy consumption.

The second routine is to utilize a surrogate gradient function, which constitutes a continuous relaxation of the non-smooth spiking during BP, to enable standard BP or BPTT for training an SNN from scratch. Direct training algorithms appear to be diverse in the selection of gradient functions [Wu *et al.*, 2018; Nefci *et al.*, 2019] and coding schemes [Zhang *et al.*, 2020; Zhou *et al.*, 2021]. Compared to the converted SNNs, the directly trained SNNs have a great advantage in the number of time steps, which can be particularly appealing for the implementation on power-efficient neuromorphic hardware. Moreover, they take neuronal dynamics into further consideration during training and the capability for processing spatiotemporal event-stream data is always regarded as a critical measurement. Unfortunately, the shallow structures of the current directly trained SNNs obstruct further exploration on large-scale datasets and in complex tasks. Zheng *et*

*al.* propose TDBN to alleviate the problem and firstly obtain directly trained ResNet-34/50, but there is a lack of discussion about how helpful this method can be for deepening the network and their results are not satisfying enough compared to the converted SNNs or ANNs. We also notice a contemporaneous work that looks into deep residual SNNs [Fang *et al.*, 2021] by adding element-wise operations into two spiking branches within a res-block. Their method is similar but orthogonal to ours.

### 2.2 Residual Learning

Theoretical and empirical evidences indicate that the depth of neural networks is crucial for their success, but the training becomes more difficult as the depth increases [Srivastava *et al.*, 2015]. Starting with ResNet [He *et al.*, 2016a; He *et al.*, 2016b], the shortcut connection is introduced as an additional branch for an unimpeded flow of both information and its gradient. It is widely adopted in later works, such as DenseNet [Huang *et al.*, 2017], Inception-ResNet [Szegedy *et al.*, 2017], and Transformer [Vaswani *et al.*, 2017]. One explanation for its superiority is that ResNet works as an implicit ensemble of numerous shallower networks [Veit *et al.*, 2016]. In addition, via the perspective of dynamical mean field theory, ResNet is proved to achieve dynamical isometry in a universal way [Tarnowski *et al.*, 2019]. Obviously, residual learning has gone beyond the ResNet structure and becomes a key component in the network architecture design. It has been utilized in the converted SNNs but remains challenging in the directly trained SNNs. In our work, the drawbacks of adopting canonical ResNet in SNNs are revealed and an improved spiking residual block is proposed.

## 3 Preliminaries and Motivation

### 3.1 Preliminaries of SNNs

The basic differences between an SNN and an ANN originate from their primary computing element, i.e., the neuron. In ANNs, a biological neuron is abstracted as an information aggregation unit with a nonlinear transformation. Meanwhile in SNNs, the neuronal dynamics of the membrane potential and the spiking communication scheme are more closely mimicked. In this work, we select the iterative LIF model proposed by Wu *et al.*, which is formulated as

$$u_i^t = \tau_{mem} \cdot u_i^{t-1} + \sum_{j=1}^n w_{ij} o_j^t, \quad (1)$$

$$o_i^t = g(u_i^t) = \begin{cases} 1, & u_i^t - V_{th} \geq 0 \\ 0, & u_i^t - V_{th} < 0 \end{cases}, \quad (2)$$

where  $u_i^t$  is the membrane potential of the  $i^{th}$  neuron in a layer at time step  $t$ ,  $\tau_{mem}$  is a decay factor for leakage and the synaptic input is the weighted sum of output spikes from the previous layer.  $g(\cdot)$  describes the firing activity controlled by the threshold  $V_{th}$  and  $u_i^t$  will be subsequently reset to  $V_{reset}$  once a spike fires. The surrogate gradient is defined as

$$\frac{\partial o_i^t}{\partial u_i^t} = \frac{1}{a} \text{sign}(|u_i^t - V_{th}| \leq \frac{a}{2}). \quad (3)$$

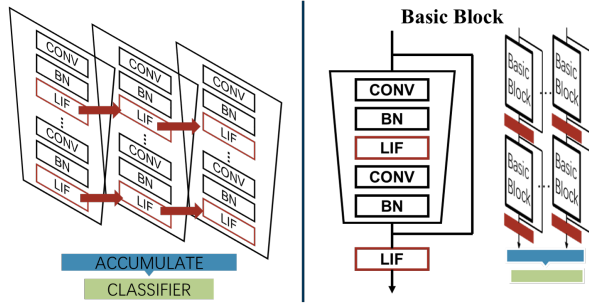


Figure 1: PlainNet and vanilla ResNet in SNNs.

The coefficient  $a$  is introduced to ensure that the integral of the function is 1. In this way, BPTT can be carried out along with the autograd framework of current deep learning libraries.

### 3.2 Transplantation of ResNet and Degradation

For computer vision tasks, a stacking of {Conv-BN-Nonlinearity} is a universal architecture which follows the primary philosophy of VGG network, and is referred to as PlainNet in this work. We adopt TDBN technique [Zheng *et al.*, 2021] as BN in our spiking models and formulate it as

$$u_i^t = \tau_{mem} u_i^{t-1} + TDBN(I_i^t, \mu_{c_i}, \sigma_{c_i}^2, V_{th}), \quad (4)$$

where  $\mu_{c_i}, \sigma_{c_i}^2$  are channel-wise mean and variation calculated per-dimension over a mini-batch of the sequential input  $\{I_i^t = \sum_{j=1}^n w_{ij} o_j^t | t = 1, \dots, T\}$ .

The direct transplantation of the residual block from non-spiking ResNet is shown in Figure ??, which is a conventional practice in previous works [Sengupta *et al.*, 2019; Hu *et al.*, 2018; Stöckl and Maass, 2021]. A shortcut connection is inserted into PlainNet and turns it into its residual counterpart, which can be written as

$$o^l = LIF(\mathcal{F}(o^{l-1}; \mathbf{W}^l) + o^{l-1}), \quad (5)$$

where  $\mathcal{F}(\cdot)$  represents the group of functions in a residual path with  $\mathbf{W}^l$  as their weight parameters,  $o^l$  is the overall firing pattern over a simulation period and  $l, l-1$  represent the layer index.

The most straightforward way of training higher quality models is by increasing their size, especially given the availability of a large amount of labeled training data [Szegedy *et al.*, 2015]. However, directly deepening network has never seemed to be a trustworthy approach to more satisfying accuracy in the field of SNNs.

We would firstly explore the extend to which the BN technique and shortcut connections have helped with the scalability of spiking models. Therefore, experiments on CIFAR-10 [Krizhevsky and Hinton, 2009] are conducted with varying depth only, and it should be noted that our focus is on the response of a network to its depth and potential degradation problem rather than pushing the state-of-the-art results, so we intentionally use deep but relatively narrow architectures as in Table 1. Table 2 shows the results of depth analysis.

Layers	$1 + 2n$	$2n$	$2n$
Output Size	32x32	16x16	8x8
Channels	16	32	64

Table 1: The structure for depth analysis on CIFAR-10.

The accuracy of PlainNet with BN begins to drop at the depth of 14 layers, and surprisingly the adoption of shortcut connections will just shift the peak to a depth of 20 layers. Despite a gentler slope after the peak, severe accuracy loss occurs in spiking ResNet when the depth reaches over 56 layers. The degradation problem still exists in spite of the introduction of BN and shortcut connections, indicating that the direct transplantation of ResNet to SNNs does not work appropriately and making building sufficiently deep and powerful SNN models a nontrivial task. Interestingly, we have noticed that the degradation problem could be alleviated within the depth of 56 layers when we remove the spiking activation functions  $LIF(\cdot)$  between residual blocks and maintain those in the residual paths as nonlinearity. Based on this observation, we mainly identify the crux of degradation as the interblock  $LIF(\cdot)$ , and will provide further insight into it with our proposed architecture in the next section.

Depth	8	14	20	32	44	56
PlainNet	81.1	85.2	83.7	76.4	59.5	N/A
ResNet	81.5	85.9	86.7	85.4	84.6	72.4
W/O $LIF(\cdot)$	80.0	86.9	88.2	88.8	89.4	90.0
<b>Our work</b>	82.0	87.4	88.4	89.7	90.0	90.4

Table 2: Depth analysis on CIFAR-10.

## 4 Spiking Residual Blocks

In this section, we will try to explain why the interblock  $LIF(\cdot)$  obstructs the applicability of vanilla ResNet in the specifics of SNNs' characteristics, introduce the corresponding superiority of our model as well as some other concerns about the new block design. The model's advantages are threefold:

- An unimpeded inference flow which can avoid unavail- ing residual expression and imbalanced workload,
- Achieving dynamic isometry which is an important met- ric to avoid gradient vanishing or explosion problem,
- Primary energy-efficient features which are intentionally maintained and will suit for further implementation on neuromorphic hardware.

The spiking residual block we proposed is illustrated in Fig- ure 2. The interlayer  $LIF(\cdot)$  is removed to construct a short- cut that goes throughout the whole network and mainly deals with the confluences of synaptic input from different residual paths. Meanwhile an additional  $LIF(\cdot)$  is placed at the top of the residual path to convert messages into sparse spikes and send them to subsequent neurons. What flows in the shortcut is conceptually closer to membrane potentials rather

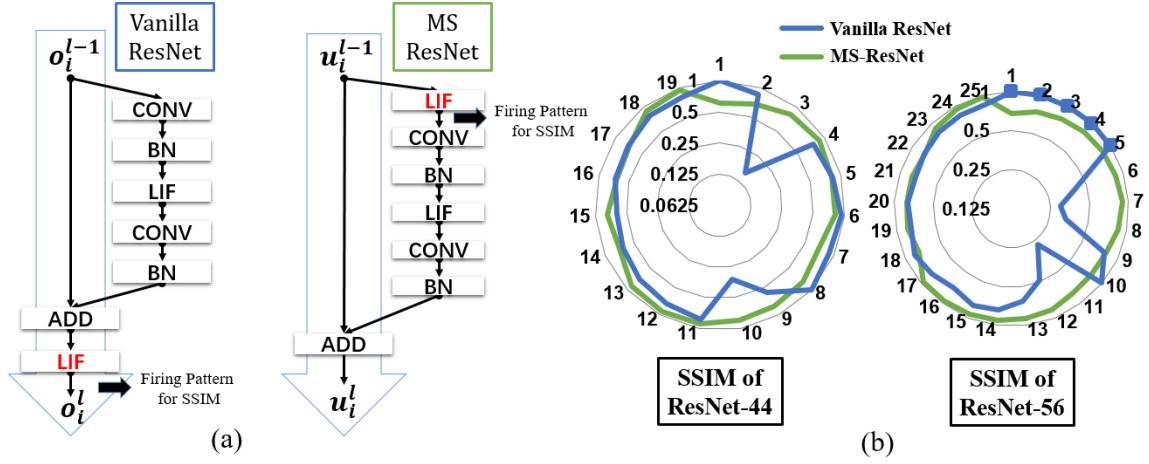


Figure 2: (a) Basic blocks in vanilla spiking ResNet and MS-ResNet. (b) The SSIM radar chart of ResNet-44 and ResNet-56.

than spiking activities in the original structure. So we name the new structure as the Membrane-Shortcut ResNet (MS-ResNet) to emphasize the change to the shortcut.

#### 4.1 Residual Representation and Workload Balance at inference

In vanilla ResNet, since the final output of a residual block is its firing pattern, we regard the change between two firing patterns at the beginning and end of a block as its effect on information processing. Then, the weakness of the original structure will gradually be reflected in the answer to the following question. What if we want an instant change to a neuron’s firing state after receiving messages from a residual block, i.e.  $S = \{s_i = (o_i^{t,l}, o_i^{t,l+1}) \mid o_i^{t,l} + o_i^{t,l+1} = 1, o_i^t \in \{0, 1\}\}$ ?

The probability of a successful change to the firing pattern can be decomposed into two conditions, which can be rewritten as

$$\begin{aligned}
 P(s_i \in S) &= P(s_i = (0, 1)) + P(s_i = (1, 0)) \\
 &= P(\mathcal{F}(o_i^l; \mathbf{W}_i^{l+1}) > V_{th} \mid o_i^l = 0) P(o_i^l = 0) \\
 &\quad + P(\mathcal{F}(o_i^l; \mathbf{W}_i^{l+1}) + 1 < V_{th} \mid o_i^l = 1) P(o_i^l = 1), \tag{6}
 \end{aligned}$$

where the part of decayed membrane potential is omitted here for simplicity. Assume the synaptic input the neuron receives at the bottom of a residual block is normally distributed  $\mathcal{F}(o_i^l; \mathbf{W}_i^{l+1}) \sim \mathcal{N}(0, \sigma_x^2)$ . With variance  $\sigma_x^2 = V_{th}^2 = 0.25$  (a representative value adopted from Zheng *et al.*), we have  $P(\mathcal{F}(o_i^l) > V_{th} \mid o_i^l = 0) = P(\mathcal{F}(o_i^l) + 1 < V_{th} \mid o_i^l = 1) = \varphi(x \geq 1) = \int_{-\infty}^1 \frac{1}{\sqrt{2\pi}} e^{-\frac{x^2}{2}} \approx 16\%$ . The values of the conditional probabilities indicate that the information conveyed through the residual path has to be strong and distinct enough to effectively influence the identity shortcut. Otherwise the firing pattern will not change when passing through the residual block. To make things worse, the increment the residual path contributes will be forgotten for those firing neurons due to the reset mechanism, which makes the residual representation of this block totally in vain in both spatial and temporal

dimension. Basically, in residual learning we would like the residual path to learn the relatively small perturbation with reference to an identity mapping, however the transplantation of ResNet in SNNs can not meet this objective due to discrete spikes and the threshold mechanism.

For RM-ResNet, the identity mapping is not constrained to the discrete spiking activity and the small residual representation can always be accumulated as

$$\begin{aligned}
 \mathbf{I}^l &= \mathbf{I}^{l-1} + \mathcal{F}(\text{LIF}(\mathbf{I}^{l-1}; \mathbf{W}^l)) \\
 &= \mathbf{I}^1 + \sum_{l=2}^L \mathcal{F}(\text{LIF}(\mathbf{I}^{l-1}; \mathbf{W}^l)), \tag{7}
 \end{aligned}$$

where  $\mathbf{I}^l$  represents the synaptic input of  $l$ -th layer. The removing of the interblock  $\text{LIF}(\cdot)$  can provide a clean path for the information flow.

To give a more intuitive verification about how firing patterns may change along with residual blocks of different layers, we adopt structural similarity index measure (SSIM) to quantify the similarity between them, which can be formulated as

$$\text{SSIM}(x, y) = \frac{(2\mu_x\mu_y + C_1)(2\sigma_{xy} + C_2)}{(\mu_x^2 + \mu_y^2 + C_1)(\sigma_x^2 + \sigma_y^2 + C_2)}, \tag{8}$$

with  $\mu_x, \sigma_x^2, \mu_y, \sigma_y^2$  the mean and variance of image  $x$  and  $y$ ,  $\sigma_{xy}$  the covariance of  $x$  and  $y$ , and  $C_1, C_2$  two constant variables. The pixel-value of an image is defined as the firing rate of a neuron in rate coding scheme and the sampling point is illustrated in Figure 2. The value of SSIM ranges from -1 and +1, and only equals +1 if the two images are identical.

If the firing pattern changes uniformly between layers, it will appear as a circle in the radar chart of Figure 2. Although a strict circle does not seem to be applicable for the whole neural network due to downsampling layers, our RM-ResNet has shown a rounder curve than vanilla spiking ResNet. Especially, there are 5 layers with an SSIM value of +1 in vanilla ResNet-56, which implies that the firing patterns do not change when the information flows through the residual

blocks and that these layers fail to help with feature extraction. Consequently, a following layer needs to compensate for the inaction of preceding layers, and it is shown as an ensuing dramatic information change. The workload of the whole network is unbalanced especially when it comes to the training of deep networks, which undoubtedly reflects the irrationality of the spiking ResNet, while RM-ResNet has effectively alleviated this unbalance.

## 4.2 Gradient Evolvement at backpropagation

Dynamical isometry, the equilibration of singular values of the input-output Jacobian matrix, has been developed in recent years as a theoretical explanation of well-behaved neural networks. In this subsection, we analyze with block dynamical isometry framework that RM-ResNet can achieve gradient norm equality while the vanilla spiking ResNet cannot.

Without loss of generality, a neural network can be viewed as a serial of blocks:

$$f(x_0) = f_{\theta^L}^L \circ f_{\theta^{L-1}}^{L-1} \circ \dots \circ f_{\theta^1}^1(x_0) \quad (9)$$

where  $\theta^i$  is the parameter matrix of the  $i$ -th layer. For the sake of simplicity, we denote  $\frac{\partial f^j}{\partial f^{j-1}} = J_j$ . Let  $\phi(J)$  be the expectation of  $tr(J)$  and  $\varphi(J)$  be  $\phi(J^2) - \phi(J)^2$ .

**Definition 1** (Block Dynamical Isometry). *Consider a neural network that can be represented as Equation 9 and the  $j$ -th block's Jacobian matrix is denoted as  $J_j$ . If  $\forall j$ ,  $\phi(J_j J_j^T) \approx 1$  and  $\varphi(J_j J_j^T) \approx 0$ , the network achieves block dynamical isometry.*

**Lemma 1.** *Assuming that for each of  $L$  sequential blocks in a neural network, we have  $\phi(J_i J_i^T) = \omega + \tau \phi(\widetilde{J_i J_i^T})$  where  $J_i$  is its Jacobian matrix. Given  $\lambda \in \mathbb{N}^+ < L$ , if  $C_L^\lambda (1 - \omega)^\lambda$  and  $C_L^\lambda \tau^\lambda$  are small enough, the network would be as stable as a  $\lambda$ -layer network when both networks have  $\forall i$ ,  $\phi(J_i J_i^T) \approx 1$ .*

Based on Definition 1 and Lemma 1, we can judge whether a network can achieve gradient norm equality in the specifics of SNNs.

**Proposition 1.** *The vanilla spiking ResNet does not achieve block dynamical isometry while the basic block of RM-ResNet could be as stable as a 1-layer network which satisfies  $\phi(J_i J_i^T) \approx 1$ .*

*Proof.* It is detailed in **Supplementary Material**.  $\square$

## 4.3 Spike-based convolution

It should be pointed out that ResNet without interblock  $LIF(\cdot)$  is also undesired for SNNs. One main source of energy efficiency for neuromorphic computing is the spike-based convolution, which means that the convolutional layer receives and processes the binary spiking input and it is feasible to replace the multiply-and-accumulate (MAC) operations in ANNs with spike-driven synaptic accumulate (AC) operations in SNNs. Specialized optimization, for example the look up table, can be applied to further boost its efficiency [Liang *et al.*, 2021]. Once  $LIF(\cdot)$  is removed, the CONV at the top of the next block will receive the continuous input

rather than binary spikes, causing difficulty in benefiting from spike-based convolution and rich input/output sparsity.

In addition, only removing the interblock  $LIF(\cdot)$  will, in effect, make the convolutional layer in the residual path connected with the one at the top of its subsequent block, and weaken their feature extraction ability. It turns out that the accuracy of W/O  $LIF(\cdot)$  will be lower than the vanilla model before the degradation problem occurs. Therefore, we place an extra  $LIF(\cdot)$  at the top of the residual path in order to maintain spike-based convolution as well as fully utilize the convolutional layers.

## 4.4 Depth Analysis on CIFAR-10

We carry out the depth analysis experiment on CIFAR-10 with MS-ResNet as well. The results are shown in Table 3, which indicates that our MS-ResNet can expand to a large scale without facing the degradation problem while preserving its accuracy in shallow structures. Besides, we set  $n$  to 36, 80 to obtain extremely deep MS-ResNet110, MS-ResNet482 on CIFAR10 with test accuracy of 91.7% and 91.9% respectively. Although the improvement in accuracy is not significant due to increasingly prominent overfitting problem (the regularization method in this experiment maintains the same), it surely evidences the scalability and the capability of our model to avoid degradation.

# 5 Experiments

## 5.1 ImageNet

### Experimental Setup

We evaluate our models on the ImageNet 2012 dataset [Deng *et al.*, 2009]. The models are trained with the 1.28 million training images and tested with the 50k validation images. The training recipe at first simply follows that of He *et al.* for our SRM-ResNet18 and SRM-ResNet34, i.e., a  $224 \times 224$  random crop with horizontal flip for data augmentation and a SGD optimizer with a weight decay of  $1e-4$  and a momentum of 0.9. However, the model would suffer from severe overfitting when it is extended to a depth of 104 layers. Despite accuracy improvement on the validation set, its training accuracy improves by a significantly larger margin. We hypothesize that this is because MS-ResNet104 has much higher model capacity. To fully unleash the potential of the deep spiking model SRM-ResNet104, an advanced training recipe is taken with stronger data augmentation and stronger regularization (See **Supplementary Material** for more training details).

### Results

As the network deepens, a satisfyingly increasing tendency of accuracy has been observed and the great scalability of our model has been evidenced (Table 3). It shows the effectiveness of  $LIF(\cdot)$  working in the residual paths as activation functions, despite spike-based computation required, and clearly demonstrates the potential of deepening SNN models.

When compared with other advanced works, our ResNet-34 with an accuracy of **69.42%** surpasses all previous directly trained SNNs at the same depth, and our ResNet-104 with an accuracy of **74.21%** is even comparable to the converted

Method	Work	Model	Time step	Acc.(%)
<b>ANN Conversion</b>	[Sengupta <i>et al.</i> , 2019]	VGG-16	2500	69.96
		ResNet-34		65.47
	[Han <i>et al.</i> , 2020]	VGG-16	4096	73.09
		ResNet-34		69.89
	[Hu <i>et al.</i> , 2018]	ResNet-34	350	71.61
		ResNet-50		72.75
[Stöckl and Maass, 2021]†	ResNet-50	500	75.10	
<b>Hybird Training</b>	[Rathi <i>et al.</i> , 2020]	VGG-16	250	65.19
		ResNet-34		61.48
<b>Direct Training</b>	[Zheng <i>et al.</i> , 2021]	ResNet-50	6	64.88
		Wide-ResNet-34		67.05
	[Fang <i>et al.</i> , 2021]	ResNet-34	4	67.04
		ResNet-50		67.78
		ResNet-101		68.76
<b>Direct Training</b>	<b>Our Work SRM-ResNet</b>	ResNet-18	6	63.10
		ResNet-34		69.42
		ResNet-104	5	<b>74.21</b>
		ResNet-104*		<b>76.02</b>
<b>Backpropagation</b>	ANN	ResNet-18	/	69.76
		ResNet-34	/	73.30
		ResNet-104‡	/	<b>76.87</b>

Table 3: ImageNet results. †A spike is allowed to carry multi-bit information. ‡Since ResNet-104 is not a standard ResNet model, we train its ANN counterpart under the same recipe. \*The input crops are enlarged to  $288 \times 288$  in inference.

SNNs in spite of much fewer time steps required for an inference. An accuracy gap to ANNs of about 2.6% is close to those of multi-timesteps converted SNNs and we also find that just enlarging the images for inference from  $224 \times 224$  to  $288 \times 288$  can improve the accuracy to a more competitive score at 76.02%.

Work	Method	Params	Acc.(%)
[Ramesh <i>et al.</i> , 2020]	DART	N.A.	65.78
[Kugele <i>et al.</i> , 2020]	Rollout-ANN	0.5M	66.75
[Zheng <i>et al.</i> , 2021]	Spiking ResNet-19	12.6M	67.80
[Yao <i>et al.</i> , 2021]	TA-SNN	1.7M	72.00
[Fang <i>et al.</i> , 2020]	PLIF	1.5M	74.80
<b>Our work</b>	<b>SRM-ResNet20</b>	0.27M	<b>75.56</b>

Table 4: Results on CIFAR10-DVS.

## 5.2 CIFAR10-DVS

### Experimental Setup

CIFAR10-DVS is an event-stream dataset for object classification [Li *et al.*, 2017]. 10,000 frame-based images from CIFAR-10 are recorded by a dynamic vision sensor (DVS) and converted into event streams. We take the dataset to test our models for their capability of spatiotemporal processing and adopt the same data preprocessing in Fang *et al.*

### Results

Our ResNet-20 achieves a new record on CIFAR10-DVS (Table 4). The model mainly follows the deep but narrow paradigm in Table 1 except that an additional downsampling is placed at the first convolution stage due to the larger input size. Our model, despite its depth, actually has a smaller

amount of parameters compared with other works, which is about one-sixth of those in Yao *et al.* and Fang *et al.*

Model	32bit-FP: MAC 4.6pJ		AC 0.9pJ	
	G-FLOPs	E(ANN) (1E-3J)	G-SyOPs	E(SNN) (1E-3J)
ResNet-34	3.53	16.22	4.77	4.29
ResNet-104	11.79	54.24	11.32	10.19

Table 5: Energy consumption for a single ImageNet image.

## 5.3 Energy Efficiency Estimation

Great sparsity is observed in MS-ResNet. The firing rates of MS-ResNet34 and MS-ResNet104, defined as the firing probability of each neuron per time step, are **0.225** and **0.192**, respectively.

To further demonstrate the energy efficiency, we estimate the energy cost based on the number of operations and the data for various operations in 45nm technology [Horowitz, 2014]. We focus solely on convolutional layers in the residual paths, which constitute a major part of floating-point operations (FLOPs). With the sparsity of spikes and short simulation process, MS-ResNet can achieve the calculation of the residual part with about the same number of synaptic operations (SyOPs) rather than FLOPs (Table 5), which means that **each neuron emits only one spike on average**.

## 6 Conclusion

In this work, we propose a novel spiking residual block to tackle the degradation problem, which enables the direct training of a 482-layer model on CIFAR-10 and a 104-layer

model on ImageNet. The great depth brings superior representation power. To our best knowledge, this is the first time such high performance is reported on ImageNet with directly trained SNNs. In addition, our resulting models attain vary sparse spiking activities and extremely low latency, indicating remarkable energy efficiency especially for spatiotemporal information processing. A deep and powerful SNN model is surely to work as the backbone for our further exploration in brain-inspired computing.

## A Appendix

### References

- [Akopyan *et al.*, 2015] Filipp Akopyan, Jun Sawada, Andrew Cassidy, Rodrigo Alvarez-Icaza, John Arthur, Paul Merolla, Nabil Imam, Yutaka Nakamura, Pallab Datta, Gi-Joon Nam, Brian Taba, Michael Beakes, Bernard Brezzo, Jente B. Kuang, Rajit Manohar, William P. Risk, Bryan Jackson, and Dharmendra S. Modha. Truenorth: Design and tool flow of a 65 mw 1 million neuron programmable neurosynaptic chip. *IEEE Transactions on Computer-Aided Design of Integrated Circuits and Systems*, 34(10):1537–1557, 2015.
- [Davies *et al.*, 2018] Mike Davies, Narayan Srinivasa, Tsung-Han Lin, Gautham Chinya, Yongqiang Cao, Sri Harsha Choday, Georgios Dimou, Prasad Joshi, Nabil Imam, Shweta Jain, Yuyun Liao, Chit-Kwan Lin, Andrew Lines, Ruokun Liu, Deepak Mathaikutty, Steven McCoy, Arnab Paul, Jonathan Tse, Guruguhanathan Venkataramanan, Yi-Hsin Weng, Andreas Wild, Yoonseok Yang, and Hong Wang. Loihi: A neuromorphic many-core processor with on-chip learning. *IEEE Micro*, 38(1):82–99, 2018.
- [Deng *et al.*, 2009] Jia Deng, Wei Dong, Richard Socher, Li-Jia Li, Kai Li, and Li Fei-Fei. Imagenet: A large-scale hierarchical image database. In *2009 IEEE Conference on Computer Vision and Pattern Recognition*, pages 248–255, 2009.
- [Deng, 2012] Li Deng. The mnist database of handwritten digit images for machine learning research [best of the web]. *IEEE Signal Processing Magazine*, 29(6):141–142, 2012.
- [Fang *et al.*, 2020] Wei Fang, Zhaofei Yu, Yanqi Chen, Timothee Masquelier, Tiejun Huang, and Yonghong Tian. Incorporating learnable membrane time constant to enhance learning of spiking neural networks, 2020.
- [Fang *et al.*, 2021] Wei Fang, Zhaofei Yu, Yanqi Chen, Tiejun Huang, Timothée Masquelier, and Yonghong Tian. Deep residual learning in spiking neural networks, 2021.
- [Han *et al.*, 2020] Bing Han, Gopalakrishnan Srinivasan, and Kaushik Roy. Rmp-snn: Residual membrane potential neuron for enabling deeper high-accuracy and low-latency spiking neural network. In *Proceedings of the IEEE/CVF Conference on Computer Vision and Pattern Recognition (CVPR)*, June 2020.
- [He *et al.*, 2016a] Kaiming He, Xiangyu Zhang, Shaoqing Ren, and Jian Sun. Deep residual learning for image recognition. In *Proceedings of the IEEE Conference on Computer Vision and Pattern Recognition (CVPR)*, June 2016.
- [He *et al.*, 2016b] Kaiming He, Xiangyu Zhang, Shaoqing Ren, and Jian Sun. Identity mappings in deep residual networks. In Bastian Leibe, Jiri Matas, Nicu Sebe, and Max Welling, editors, *Computer Vision – ECCV 2016*, pages 630–645, Cham, 2016. Springer International Publishing.
- [Horowitz, 2014] Mark Horowitz. 1.1 computing’s energy problem (and what we can do about it). In *2014 IEEE International Solid-State Circuits Conference Digest of Technical Papers (ISSCC)*, pages 10–14, 2014.
- [Hu *et al.*, 2018] Yangfan Hu, Huajin Tang, and Gang Pan. Spiking deep residual network. *arXiv preprint arXiv:1805.01352*, 2018.
- [Huang *et al.*, 2017] Gao Huang, Zhuang Liu, Laurens van der Maaten, and Kilian Q. Weinberger. Densely connected convolutional networks. In *Proceedings of the IEEE Conference on Computer Vision and Pattern Recognition (CVPR)*, July 2017.
- [Kim *et al.*, 2020] Seijoon Kim, Seongsik Park, Byunggook Na, and Sungroh Yoon. Spiking-yolo: Spiking neural network for energy-efficient object detection. *Proceedings of the AAAI Conference on Artificial Intelligence*, 34(07):11270–11277, Apr. 2020.
- [Krizhevsky and Hinton, 2009] Alex Krizhevsky and Geoffrey Hinton. Learning multiple layers of features from tiny images. 2009.
- [Kugele *et al.*, 2020] Alexander Kugele, Thomas Pfeil, Michael Pfeiffer, and Elisabetta Chicca. Efficient processing of spatiotemporal data streams with spiking neural networks. *Frontiers in Neuroscience*, 14:439, 2020.
- [Lee *et al.*, 2020] Chankyu Lee, Adarsh Kumar Kosta, Alex Zihao Zhu, Kenneth Chaney, Kostas Daniilidis, and Kaushik Roy. Spike-flownet: Event-based optical flow estimation with energy-efficient hybrid neural networks. In Andrea Vedaldi, Horst Bischof, Thomas Brox, and Jan-Michael Frahm, editors, *Computer Vision – ECCV 2020*, pages 366–382, Cham, 2020. Springer International Publishing.
- [Li *et al.*, 2017] Hongmin Li, Hanchao Liu, Xiangyang Ji, Guoqi Li, and Luping Shi. Cifar10-dvs: An event-stream dataset for object classification. *Frontiers in Neuroscience*, 11:309, 2017.
- [Liang *et al.*, 2021] Ling Liang, Zheng Qu, Zhaodong Chen, Fengbin Tu, Yujie Wu, Lei Deng, Guoqi Li, Peng Li, and Yuan Xie. H2learn: High-efficiency learning accelerator for high-accuracy spiking neural networks. *arXiv preprint arXiv:2107.11746*, 2021.
- [Maass, 1997] Wolfgang Maass. Networks of spiking neurons: The third generation of neural network models. *Neural Networks*, 10(9):1659–1671, 1997.
- [Mayr *et al.*, 2019] Christian Mayr, Sebastian Hoepfner, and Steve Furber. Spinnaker 2: A 10 million core processor system for brain simulation and machine learning. *arXiv preprint arXiv:1911.02385*, 2019.
- [Neftci *et al.*, 2019] Emre O. Neftci, Hesham Mostafa, and Friedemann Zenke. Surrogate gradient learning in spiking neural networks: Bringing the power of gradient-based optimization to spiking neural networks. *IEEE Signal Processing Magazine*, 36(6):51–63, 2019.
- [Pei *et al.*, 2019] Jing Pei, Lei Deng, Sen Song, Mingguo Zhao, Youhui Zhang, Shuang Wu, Guanrui Wang, Zhe Zou, Zhenzhi Wu, Wei He, Feng Chen, Ning Deng, Si Wu, Yu Wang, Yujie Wu, Zheyu Yang, Cheng Ma, Guoqi Li, Wentao Han, Huanglong Li, Huaqiang Wu, Rong Zhao, Yuan Xie, and Luping Shi. Towards artificial general intelligence with hybrid tianjic chip architecture. *Nature*, 572(7767):106–111, 2019.
- [Ramesh *et al.*, 2020] Bharath Ramesh, Hong Yang, Garrick Orchard, Ngoc Anh Le Thi, Shihao Zhang, and Cheng Xiang. Dart: Distribution aware retinal transform for event-based cameras. *IEEE Transactions on Pattern Analysis and Machine Intelligence*, 42(11):2767–2780, 2020.

- [Rathi *et al.*, 2020] Nitin Rathi, Gopalakrishnan Srinivasan, Priyadarshini Panda, and Kaushik Roy. Enabling deep spiking neural networks with hybrid conversion and spike timing dependent backpropagation. In *International Conference on Learning Representations*, 2020.
- [Rueckauer *et al.*, 2017] Bodo Rueckauer, Iulia-Alexandra Lungu, Yuhuang Hu, Michael Pfeiffer, and Shih-Chii Liu. Conversion of continuous-valued deep networks to efficient event-driven networks for image classification. *Frontiers in Neuroscience*, 11:682, 2017.
- [Sengupta *et al.*, 2019] Abhronil Sengupta, Yuting Ye, Robert Wang, Chiao Liu, and Kaushik Roy. Going deeper in spiking neural networks: Vgg and residual architectures. *Frontiers in Neuroscience*, 13:95, 2019.
- [Srivastava *et al.*, 2015] Rupesh Kumar Srivastava, Klaus Greff, and Jürgen Schmidhuber. Training very deep networks. In *Proceedings of the 28th International Conference on Neural Information Processing Systems - Volume 2, NIPS'15*, page 2377–2385, Cambridge, MA, USA, 2015. MIT Press.
- [Stöckl and Maass, 2021] Christoph Stöckl and Wolfgang Maass. Optimized spiking neurons can classify images with high accuracy through temporal coding with two spikes. *Nature Machine Intelligence*, 3(3):230–238, 2021.
- [Szegedy *et al.*, 2015] Christian Szegedy, Wei Liu, Yangqing Jia, Pierre Sermanet, Scott Reed, Dragomir Anguelov, Dumitru Erhan, Vincent Vanhoucke, and Andrew Rabinovich. Going deeper with convolutions. In *Proceedings of the IEEE Conference on Computer Vision and Pattern Recognition (CVPR)*, June 2015.
- [Szegedy *et al.*, 2017] Christian Szegedy, Sergey Ioffe, Vincent Vanhoucke, and Alexander A. Alemi. Inception-v4, inception-resnet and the impact of residual connections on learning. In *Proceedings of the Thirty-First AAAI Conference on Artificial Intelligence, AAAI'17*, page 4278–4284. AAAI Press, 2017.
- [Tarnowski *et al.*, 2019] Wojciech Tarnowski, Piotr Warchoń, Stanisław Jastrzębski, Jacek Tabor, and Maciej Nowak. Dynamical isometry is achieved in residual networks in a universal way for any activation function. In Kamalika Chaudhuri and Masashi Sugiyama, editors, *Proceedings of the Twenty-Second International Conference on Artificial Intelligence and Statistics*, volume 89 of *Proceedings of Machine Learning Research*, pages 2221–2230. PMLR, 16–18 Apr 2019.
- [Vaswani *et al.*, 2017] Ashish Vaswani, Noam Shazeer, Niki Parmar, Jakob Uszkoreit, Llion Jones, Aidan N. Gomez, undefinukas Kaiser, and Illia Polosukhin. Attention is all you need. In *Proceedings of the 31st International Conference on Neural Information Processing Systems, NIPS'17*, page 6000–6010, Red Hook, NY, USA, 2017. Curran Associates Inc.
- [Veit *et al.*, 2016] Andreas Veit, Michael Wilber, and Serge Belongie. Residual networks behave like ensembles of relatively shallow networks. In *Proceedings of the 30th International Conference on Neural Information Processing Systems, NIPS'16*, page 550–558, Red Hook, NY, USA, 2016. Curran Associates Inc.
- [Wu *et al.*, 2018] Yujie Wu, Lei Deng, Guoqi Li, Jun Zhu, and Luping Shi. Spatio-temporal backpropagation for training high-performance spiking neural networks. *Frontiers in Neuroscience*, 12:331, 2018.
- [Wu *et al.*, 2019] Yujie Wu, Lei Deng, Guoqi Li, Jun Zhu, Yuan Xie, and Luping Shi. Direct training for spiking neural networks: Faster, larger, better. *Proceedings of the AAAI Conference on Artificial Intelligence*, 33(01):1311–1318, Jul. 2019.
- [Wu *et al.*, 2020] Jibin Wu, Emre Yılmaz, Malu Zhang, Haizhou Li, and Kay Chen Tan. Deep spiking neural networks for large vocabulary automatic speech recognition. *Frontiers in Neuroscience*, 14:199, 2020.
- [Yang *et al.*, 2019] Zheyu Yang, Yujie Wu, Guanrui Wang, Yukuan Yang, Guoqi Li, Lei Deng, Jun Zhu, and Luping Shi. Dashnet: A hybrid artificial and spiking neural network for high-speed object tracking. *arXiv preprint arXiv:1909.12942*, 2019.
- [Yao *et al.*, 2021] Man Yao, Huanhuan Gao, Guangshe Zhao, Dingheng Wang, Yihan Lin, Zhaoxu Yang, and Guoqi Li. Temporal-wise attention spiking neural networks for event streams classification. *arXiv preprint arXiv:2107.11711*, 2021.
- [Zhang *et al.*, 2020] Malu Zhang, Jiadong Wang, Zhixuan Zhang, Ammar Belatreche, Jibin Wu, Yansong Chua, Hong Qu, and Haizhou Li. Spike-timing-dependent back propagation in deep spiking neural networks. *arXiv preprint arXiv:2003.11837*, 2020.
- [Zheng *et al.*, 2021] Hanle Zheng, Yujie Wu, Lei Deng, Yifan Hu, and Guoqi Li. Going deeper with directly-trained larger spiking neural networks. *Proceedings of the AAAI Conference on Artificial Intelligence*, 35(12):11062–11070, May 2021.
- [Zhou *et al.*, 2021] Shibo Zhou, Xiaohua Li, Ying Chen, Sanjeev T. Chandrasekaran, and Arindam Sanyal. Temporal-coded deep spiking neural network with easy training and robust performance. *Proceedings of the AAAI Conference on Artificial Intelligence*, 35(12):11143–11151, May 2021.